Machine Learning-Based Detection Time Estimation for Molecular Communication

Zhen Cheng(✉), Heng Liu, Miaodi Chen, and Zhichao Zhang

Zhejiang University of Technology, Hangzhou 310023, China
chengzhen@zjut.edu.cn

Abstract. Molecular communication (MC) utilizes the release, diffusion and reception of molecules to transmit information. It has promising prospects in the field of drug delivery. The detection time estimation of the receiver in MC system plays important roles in the resource consumption at the receiver. Existing strategies of traditional detection time mainly focus on known channel state information (CSI). In this paper, we propose a method for estimating the detection time of the receiver in MC system with unknown CSI by using deep neural network (DNN) model. We employ the Monte Carlo simulation to capture the positions of molecules in the three-dimensional environment. The dataset is generated based on the coordinates of the molecules at each position. The numerical results show that the detection time can be accurately estimated by the DNN model which exhibits good detection and generalization abilities. In addition, the number of molecules released by the transmitter and the minimum distance between the transmitter and the boundary of the receiver have impacts on the accuracy of detection time estimation of the receiver.

Keywords: Molecular Communication · Detection Time Estimation · Machine Learning

1 Introduction

Molecular communication (MC) [1] plays a crucial role in facilitating communication among entities within biological environments. In MC systems, the molecules released by the transmitter, serving as information carriers between communication entities, can convey transmission information in the environment [2]. MC has prospects for various applications, including targeted drug delivery and environmental monitoring [3]. However, several challenges need to be addressed, such as the limited memory of the receiver and determining optimal detection time [4, 5].

In recent literatures about the detection time in MC, many researchers have studied how to determine the optimal detection time for receivers. In [6], a scheme was proposed to optimize the detection interval in order to minimize the impact of Inter-Symbol Interference (ISI). This optimization was applicable to both absorption and passive receivers. Kim et al. identified appropriate symbol interval values in two vascular models and computed the data transmission rate [7]. Chen et al. designed a modified SINAR (mSINAR),

Y. Chen et al. (Eds.): BICT 2024, LNICST 592, pp. 66–75, 2025.
https://doi.org/10.1007/978-3-031-81599-7_7

which can be used to measure the bit error ratio performance of MC systems with variable detection intervals [8]. Cheng et al. [9] employed a multi-objective optimization algorithm to identify the optimal detection time for receivers in a mobile multi-user MC system in a three-dimensional (3D) anomalous diffusion channel.

Recently, there have been growing interests in incorporating machine learning functionalities into MC systems. This integration also explored the potential benefits of employing energy-efficient algorithms for machine learning on low power devices [10]. Methods for detection signals based on machine learning were studied. Shrivastava et al. [11] proposed a method for detecting signals in mobile MC based on neural networks. Sun et al. [12] introduced a novel recurrent neural network structure aiming at learning and estimating transmitted signal sequences without prior knowledge of the channel model. In response to the challenge of lacking precise mathematical models, Lu et al. [13] integrated the principles of natural language processing into MC and presented a detector named MCFormer based on the classical Transformer model. Furthermore, machine learning was explored to many applications in entity localization of MC systems. When the accurate analytical formulas for received signals were not available, Kose et al. [14] employed a deep neural network (DNN) to detect and locate the silent entities in the two-dimensional environment in MC system.

Usually, the detection time of the receiver in MC system starts when the transmitter releases molecules [15]. Considering the molecules arrive at the receiver needs some time due to the diffusion, in order to reduce resource consumption at the receiver, the receiver can delay the detection time and starts detection after it receives the first molecule. Existing strategies of traditional detection time mainly focused on known CSI. However, when the CSI is unknown, existing traditional strategies are not effective. How to estimate the detection time in MC with unknown CSI is a challenge work which needs to be studied. In order to solve the problem, we study the detection time estimation in MC with unknown CSI based on DNN model. The main contributions of our paper are as follows:

(1) We propose a method for detection time estimation in MC with unknown CSI by using DNN model. The Monte Carlo simulation is utilized to capture the positions of molecules released by the transmitter in the 3D environment. Based on the coordinates of the molecules at each position, the data generation is implemented to train the DNN model.
(2) The numerical results show that the DNN model can accurately estimate the detection time of the receiver, which demonstrates the DNN model has good detection ability and generalization ability. In addition, the impacts of the number of molecules released by the transmitter and the minimum distance between the transmitter and the receiver boundary on the accuracy of detection time estimation at the receiver are analyzed.

The remainder of this paper is organized as follows: Sect. 2 introduces the system topology, the process of data generation and the evaluation of estimation error time. Section 3 gives the simulation results about the estimation of detection time of the receiver. The conclusion is summarized in Sect. 4.

2 Machine Learning-Based Detection Time Estimation

2.1 System Topology

The system topology is consisted of a point transmitter (TX) and a spherical receiver (RX) in a static 3D and unbounded environment with no drift. The position of TX is represented by the coordinates $(x_{\mathrm{TX}}, y_{\mathrm{TX}}, z_{\mathrm{TX}})$. We assume that RX can perfectly absorb molecules. The radius of RX is represented by r and the position of RX is $(x_{\mathrm{RX}}, y_{\mathrm{RX}}, z_{\mathrm{RX}})$. The diffusion coefficient of molecules in the environment is denoted as D. It is assumed that TX and RX are synchronized in time [16]. The system model is shown in Fig. 1.

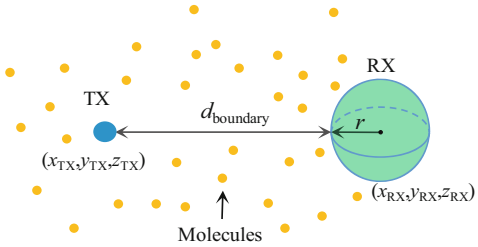

Fig. 1. System topology.

When TX releases molecules at position $(x_{\mathrm{TX}}, y_{\mathrm{TX}}, z_{\mathrm{TX}})$, the distance between TX and the boundary of RX is determined by

$$d_{\mathrm{boundary}} = \sqrt{(x_{\mathrm{TX}} - x_{\mathrm{RX}})^2 + (y_{\mathrm{TX}} - y_{\mathrm{RX}})^2 + (z_{\mathrm{TX}} - z_{\mathrm{RX}})^2} - r. \tag{1}$$

In order to ensure that the molecules will not be absorbed immediately after emission, we set the minimum distance between the transmitter and the boundary of the receiver which is d_{min}. Then we have

$$d_{\mathrm{boundary}} \geq d_{\mathrm{min}}. \tag{2}$$

2.2 Data Generation

The mechanism of estimation of the detection time is described as follows: RX estimates the detection time based on the initial coordinates of the molecules and the way that the molecules diffuse in the environment. The estimation of detection time of RX is defined by the arrival time of the first molecule when TX releases the molecules at $t = 0$. It means that RX determines whether one molecule can be captured in each time interval Δt. If no molecules are captured in this Δt, RX continues to count the molecules in subsequent Δt. Once one molecule can be captured at time t, then the time t is the detection time of RX. When the position of TX changes, the corresponding detection time of RX may vary. Therefore, it is essential to employ computer simulations to model the process of emission, motion, and absorption of molecules under different position coordinates of TX.

To enhance the accuracy of detection time estimation, we employ the Monte Carlo simulation experimental method [17] to capture the positions of molecules in the environment. In the simulation, the detection time of RX is discretely divided into multiple Δt intervals. Here Δt represents the time interval for each sampling. At time $t = 0$, TX emits N molecules. In each subsequent time interval Δt, the displacements of each molecule along the x-axis, y-axis, and z-axis are denoted by ΔX, ΔY, and ΔZ, respectively. $X(t)$, $Y(t)$ and $Z(t)$ are the coordinates of the molecules along the x-axis, y-axis, and z-axis at time t, respectively. $X(t+\Delta t)$, $Y(t+\Delta t)$ and $Z(t+\Delta t)$ are the coordinates of the molecules along the x-axis, y-axis, and z-axis at time $(t + \Delta t)$, respectively. The positional information of the molecules is updated as follows:

$$\begin{aligned} X(t+\Delta t) &= X(t) + \Delta X, \\ Y(t+\Delta t) &= Y(t) + \Delta Y, \\ Z(t+\Delta t) &= Z(t) + \Delta Z, \end{aligned} \tag{3}$$

where ΔX, ΔY and ΔZ are obtained by

$$\begin{aligned} \Delta X &= \sqrt{2D\Delta t} \times n_x, \\ \Delta Y &= \sqrt{2D\Delta t} \times n_y, \\ \Delta Z &= \sqrt{2D\Delta t} \times n_z, \end{aligned} \tag{4}$$

where n_x, n_y, and n_z are random parameters which follow an independent standard normal distribution:

$$\begin{aligned} n_x &\sim N(0, 1), \\ n_y &\sim N(0, 1), \\ n_z &\sim N(0, 1). \end{aligned} \tag{5}$$

To ensure universal applicability of the neural network, the position of TX in 3D environment needs to be randomly selected. Although the coordinates of TX can theoretically take continuous values, obtaining continuous coordinate $(x_{\mathrm{TX}}, y_{\mathrm{TX}}, z_{\mathrm{TX}})$ as training data is a challenge work due to high computational complexity. Therefore, the x-axis, y-axis, and z-axis are discretized into multiple steps and each step is 1 μm. The ranges of x_{TX}, y_{TX}, and z_{TX} are set as

$$\begin{aligned} -20\mu m \le x_{\mathrm{TX}} < 20\mu m, \\ -20\mu m \le y_{\mathrm{TX}} < 20\mu m, \\ -20\mu m \le z_{\mathrm{TX}} < 20\mu m. \end{aligned} \tag{6}$$

When TX coordinates satisfy $d_{\mathrm{boundary}} < d_{\mathrm{min}}$, the TX coordinates are not used for data generation. It is noted that the number of emitted molecules is closely linked to the range of the coordinates of TX. When the range of TX coordinates is large, the number of molecules which are emitted by TX should be sufficiently more.

Considering that x_{TX}, y_{TX}, and z_{TX} have continuous and real values, the values of x_{TX}, y_{TX}, and z_{TX} of TX at all possible positions are stored in the coordinate vectors $\boldsymbol{X}_{\mathrm{TX}}$, $\boldsymbol{Y}_{\mathrm{TX}}$, and $\boldsymbol{Z}_{\mathrm{TX}}$, respectively. The training data is consisted of distinct coordinate

vectors $\boldsymbol{X}_{\mathrm{TX}}$, $\boldsymbol{Y}_{\mathrm{TX}}$, and $\boldsymbol{Z}_{\mathrm{TX}}$. These vectors are randomly chosen coordinates within a specified range, and the values of the coordinates are uniformly distributed within the given range. This approach ensures that our model can provide good accuracy of the detection time of RX.

Based on the range of x_{TX}, y_{TX}, and z_{TX} in (6), there are 64,000 discretized coordinates in 3D environment. When $d_{\min} = 5$ µm, there are 59,861 coordinates after removing the coordinates which are not satisfied with the condition (2). For each coordinate $(x_{\mathrm{TX}}, y_{\mathrm{TX}}, z_{\mathrm{TX}})$, there are 160 training samples and 40 test samples.

2.3 Model Architecture

We employ a DNN model to estimate the detection time of RX when the CSI is unknown. After multiple testing experiments, the parameters of the DNN model are optimized. The DNN model takes three coordinate vectors of TX as input. Here, **Input1**, **Input2**, and **Input3** represent $\boldsymbol{X}_{\mathrm{TX}}$, $\boldsymbol{Y}_{\mathrm{TX}}$, and $\boldsymbol{Z}_{\mathrm{TX}}$, respectively. The output of the model is the detection time of RX, which is represented by a one-dimensional vector. In the DNN model architecture illustrated in Fig. 2, it includes four hidden layers H1, H2, H3, and H4, with each layer having 300 nodes.

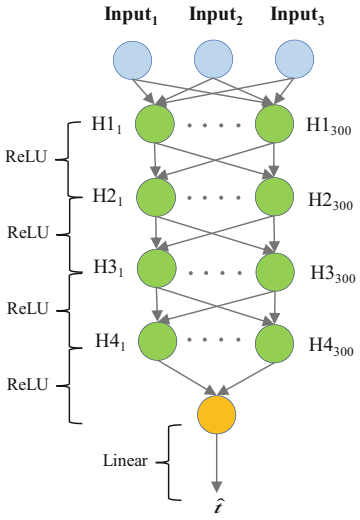

Fig. 2. The topology of the DNN model.

In the DNN model, the Rectified Linear Unit (ReLU) activation function is applied after each hidden layer to achieve nonlinearity. At the nodes in the output layer, the linear activation function is employed to compute the detection time of RX based on the corresponding topology. Given that the output of model is the predicted detection time of RX by the DNN model, the Mean Squared Error (MSE) is utilized to define the loss

function as follows:

$$L_{\mathrm{MSE}} = \frac{1}{n}\sum_{i=1}^{n}(t_i - \hat{t}_i)^2. \tag{7}$$

In (7), n is the number of training samples. t_i and $\hat{t}_i$ are represented the actual detection time and the estimated time for the i-th training sample, respectively. Throughout the training process of the utilized network model, the stochastic gradient descent (SGD) method is employed. During the optimization process of the DNN model, after numerous experiments, we set the batch size as 256 and a learning rate as 0.001. We also adopt the Adam optimizer [18] to obtain optimal results. The error of estimation detection time of RX is defined as the time difference between the estimated time from the DNN model and the arrival time of the first molecule captured by RX. This estimation error time (EET) is computed by

$$\mathrm{EET} = \left|\hat{t} - t\right|. \tag{8}$$

$\mathrm{EET}|k\Delta t$ represents the estimation error time which is at the range of k time intervals which is $k\Delta t$ ($k = 1, 2, 3, 4, 5$). $N_{\mathrm{EET}|k\Delta t}$ is the number of samples under the conditions of $\mathrm{EET}|k\Delta t$. The total number of testing dataset is N_t. The proportion of the number of error time data in $k\ \Delta t$ to the number of data in testing dataset which is denoted by PoE is computed by

$$\mathrm{PoE} = N_{\mathrm{EET}|k\Delta t}/N_t. \tag{9}$$

3 Numerical Results

According to the data generation process and the construction of the DNN model, simulation experiments are conducted by using the system parameters outlined in Table 1.

Table 1. System parameters

Symbol	Explanation	Value
D	Diffusion coefficient	$7 \times 10^{-10}\mathrm{m}^2/\mathrm{s}$
N	Number of molecules	4×10^6
Δt	Simulation time step	0.001 s
$d_{\min}$	Minimum distance between TX and the boundary of RX	5 μm
r	Radius of RX	5 μm
$(x_{\mathrm{RX}}, y_{\mathrm{RX}}, z_{\mathrm{RX}})$	The position of RX	(0,0,0)

Figure 3 shows the convergence of the DNN model on the training dataset. We can see that when a training epoch achieves 120, the output of DNN model can get better results. At this time, the variance of the value of MSE is very small.

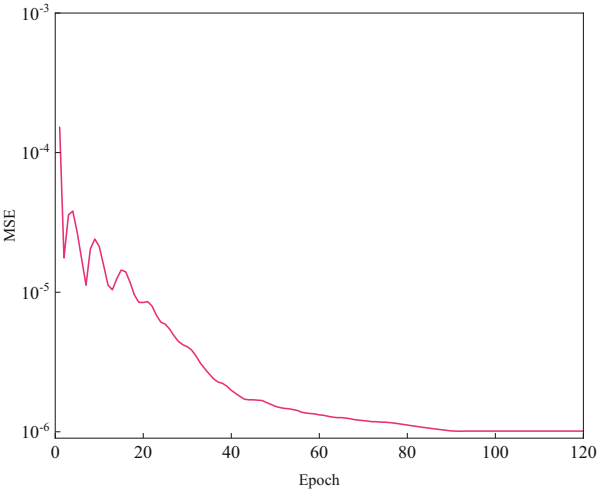

Fig. 3. MSE vs training epoch

The error data results in the testing dataset are presented in Table 2. It is evident that when the error time is within one Δt, the number of qualified testing data is more than three-quarters of the total testing dataset. Furthermore, as the estimation error time increases, the value of PoE decreases.

Table 2. PoE statistics under different ranges of EET

The statistics of estimation error time	PoE
% of Estimation error time $\leq 1\Delta t$	76.75%
% of $1\Delta t <$ Estimation error time $\leq 2\Delta t$	18.19%
% of $2\Delta t <$ Estimation error time $\leq 3\Delta t$	3.77%
% of $3\Delta t <$ Estimation error time $\leq 4\Delta t$	0.98%
% of $4\Delta t <$ Estimation error time $\leq 5\Delta t$	0.25%

In Fig. 4, we make a statistics for EET$|k\Delta t$ with $k = 1, 2, 3, 4, 5$. Then we get the value of PoE within $5\Delta t$. It is evident that the value of PoE exhibits a notable increase between one Δt and $2\Delta t$. However, when the value of PoE is within $3\Delta t$, the predicted time for the entire testing dataset closely aligns with the actual data. Notably, when the allowable error time is within $5\Delta t$, almost all the data in the testing dataset can be considered. Considering the detection time can be accurately estimated by the DNN model, it can be inferred that training on discrete points imparts generalization ability of the DNN model.

Subsequently, we employ the control variable method to conduct comparative experiments, aiming to further assess the estimation ability of the DNN model. In comparison with Fig. 4, we maintain the values of D and $d_{\min}$ while setting the number of emitted

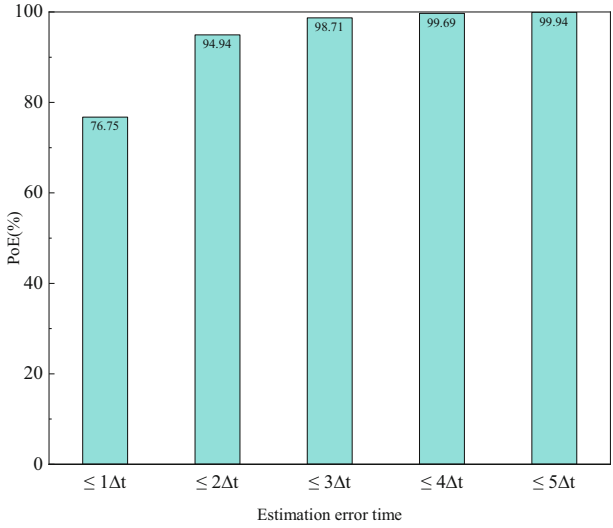

Fig. 4. The statistics of estimation error time under different values of k ($D = 7 \times 10^{-10}$ m^2/s, $\Delta t = 0.001$ s, $N = 4 \times 10^6$, $d_{\min} = 5$ μm)

molecules N to three different orders of magnitude. In addition, we keep the values of D and N constant while varying the minimum distance $d_{\min}$ between TX and the boundary of RX through three discrete values.

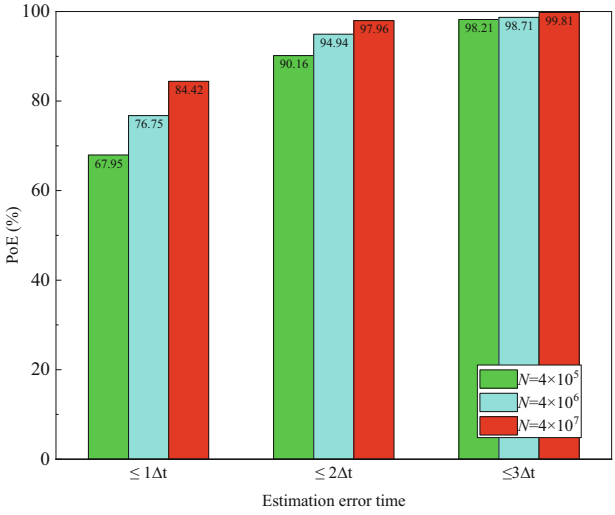

Fig. 5. The statistics of estimation error time with different values of N ($D = 7 \times 10^{-10}$ m^2/s, $\Delta t = 0.001$ s, $d_{\min} = 5$ μm)

In Fig. 5, it is observed that with an increase of the number of emitted molecules N, the value of PoE becomes more concentrated within $3\Delta t$. This phenomenon can be attributed to the fact that as the number of molecules in the environment increases, the variation of the detection time of RX is small, which makes the training of the DNN model more effective.

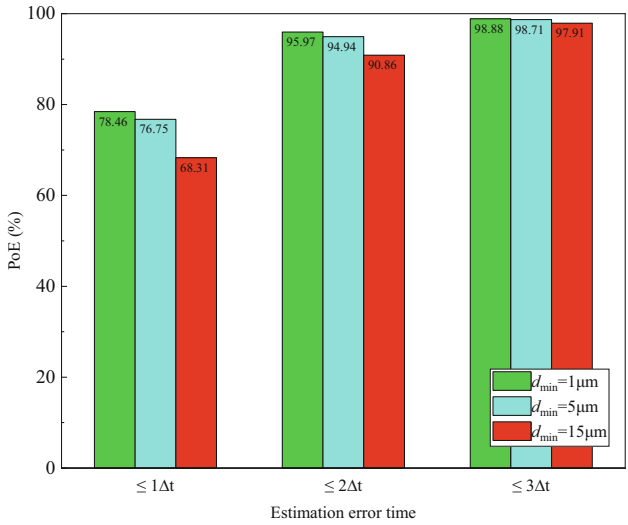

Fig. 6. The statistics of estimation error time with different values of $d_{\min}$ ($D = 7 \times 10^{-10}\text{m}^2/\text{s}$, $\Delta t = 0.001$ s, $N = 4 \times 10^6$)

In Fig. 6, when $d_{\min} = 1$ μm, some of the coordinate sets selected by TX are very close to RX. Consequently, the emitted molecules can be immediately captured by RX, which results in small variation of the detection time of capturing molecules by RX. However, when $d_{\min} = 15$ μm, the coordinate sets selected by TX are much farther from RX. In such a case, with the same number of emitted molecules, the detection time of capturing molecules by RX will have a larger variation compared with the scenarios with $d_{\min} = 1$ μm and $d_{\min} = 5$ μm. As a result, the accuracy of estimation error time by the DNN model at 15 μm is worse than those with $d_{\min} = 1$ μm and $d_{\min} = 5$ μm.

4 Conclusion

This paper proposed the use of DNN model for estimating the detection time of RX with unknown CSI. The number of molecules released by TX and the minimum distance between the transmitter and the boundary of the receiver had significant impacts on the estimation detection time of RX. Specifically, a larger number of molecules released by TX and a smaller minimum distance resulted in a more accurate estimation of the detection time of RX. In future work, we plan to explore scenarios with multiple receivers and aim to determine the detection time for each receiver in the diffusion environment with drift.

Acknowledgments. This work was supported in part by National Natural Science Foundation of China (Grant Nos. 62271446); in part by Zhejiang Provincial Natural Science Foundation of China (Grant Nos. LY23F020021).

References

1. Farsad, N., Yilmaz, H.B., Eckford, A., et al.: A comprehensive survey of recent advancements in molecular communication. IEEE Commun. Surveys Tutorials. **18**(3), 1887–1919 (2016)
2. Felicetti, L., Femminella, M., Reali, G., et al.: Applications of molecular communications to medicine: a survey. Nano Commun. Netw. **7**, 27–45 (2016)
3. Ahmadzadeh, A., Jamali, V., Schober, R.: Stochastic channel modeling for diffusive mobile molecular communication systems. IEEE Trans. Commun. **66**(12), 6205–6220 (2018)
4. Canovas-Carrasco, S., Garcia-Sanchez, A., Garcia-Haro, J.: A nanoscale communication network scheme and energy model for a human hand scenario. Nano Commun. Netw. **15**, 17–27 (2018)
5. Cao, T.N., Zlatanov, N., Yeoh, P.L., et al.: Optimal detection interval for absorbing receivers in molecular communication systems with interference. IEEE Trans. Mol. Biol. Multi-Scale Commun. **6**(3), 184–198 (2020)
6. Chen, X., Wen, M., Ji, F., et al.: Detection interval optimization for diffusion-based molecular communication. In: IEEE ICC, pp. 3691–3696. Seoul, Korea (2022)
7. Kim, N.R., Eckford, A.W., Chae, C.B.: Symbol interval optimization for molecular communication with drift. IEEE Trans. Nanobiosci. **13**(3), 223–229 (2014)
8. Chen, X., Wen, M., Ji, F., et al.: Detection interval of aerosol propagation from the perspective of molecular communication: how long is enough? IEEE J. Sel. Areas Commun. **40**(11), 3255–3270 (2022)
9. Cheng, Z., Sun, J., Zhang, Z., et al.: Optimization of detection interval for mobile multiuser molecular communication with anomalous diffusion in internet of nano things. IEEE IoT J. **11**(5), 8590–8603 (2024)
10. Balasubramaniam, S., Somathilaka, S., Sun, S., et al.: Realizing molecular machine learning through communications for biological AI. IEEE Nanotech. Mag. **17**(3), 10–20 (2023)
11. Shrivastava, A.K., Das, D., Mahapatra, R., et al.: Scaled conjugate gradient algorithm for neural network detector in mobile molecular communication. In: 2021 IEEE GLOBECOM, pp. 1–6. Madrid, Spain (2021)
12. Sun, L., Wang, Y.: CTBRNN: a novel deep-learning based signal sequence detector for communications systems. IEEE Signal Process. Lett. **27**, 21–25 (2016)
13. Lu, X., Bai, C., Zhu, A., et al.: MCFormer: a transformer-based detector for molecular communication with accelerated particle-based solution. IEEE Comm. Lett. **27**(10), 2837–2841 (2023)
14. Kose, O.D., Gursoy, M.C., Saraclar, M., et al.: Machine learning-based silent entity localization using molecular diffusion. IEEE Comm. Lett. **24**(4), 807–810 (2016)
15. Akdeniz, B.C., Pusane, A.E., Tugcu, T.: Optimal reception delay in diffusion-based molecular communication. IEEE Comm. Lett. **22**(1), 57–60 (2018)
16. Huang, L., Lin, L., Liu, F., et al.: Clock synchronization for mobile molecular communication systems. IEEE Trans. Nanobiosci. **20**(4), 406–415 (2021)
17. Arifler, D., Arifler, D.: Monte Carlo analysis of molecule absorption probabilities in diffusion-based nanoscale communication systems with multiple receivers. IEEE Trans. Nanobiosci. **16**(3), 157–165 (2017)
18. Farsad, N., Goldsmith, A.: Neural network detection of data sequences in communication systems. IEEE Trans. Signal Proces. **66**(21), 5663–5678 (2018)